

# Additive manufacturing of Co-Cr-Mo alloy: influence of heat treatment on microstructure, tribological, and electrochemical properties

Kedar Mallik Mantrala<sup>1\*</sup>, Mitun Das<sup>2</sup>, Vamsi Krishna Balla<sup>2\*</sup>, Ch. Srinivasa Rao<sup>3</sup> and V. V. S. Kesava Rao<sup>3</sup>

## OPEN ACCESS

### Edited by:

Ranji Vaidyanathan,  
Oklahoma State University, USA

### Reviewed by:

Henrique De Amorim Almeida,  
Polytechnic Institute of Leiria, Portugal  
Subhadip Bodhak,  
National Institute of Standards and  
Technology, USA

### \*Correspondence:

Kedar Mallik Mantrala,  
Department of Mechanical  
Engineering, Vasireddy Venkatadri  
Institute of Technology,  
Nambur, Guntur 522508, India  
kedarmallik@gmail.com  
Vamsi Krishna Balla,  
Bioceramics and Coating Division,  
CSIR-Central Glass and Ceramic  
Research Institute (CGCRI),  
196, Raja S. C. Mullick Road,  
Kolkata 700032, India  
vamsiballa@cgcri.res.in

### Specialty section:

This article was submitted to  
Computer-Aided and Digital  
Manufacturing Technologies,  
a section of the journal  
Frontiers in Mechanical Engineering

Received: 23 December 2014

Accepted: 16 February 2015

Published: 03 March 2015

### Citation:

Mantrala KM, Das M, Balla VK, Rao  
CS and Kesava Rao VVS. (2015)  
Additive manufacturing of Co-Cr-Mo  
alloy: influence of heat treatment on  
microstructure, tribological, and  
electrochemical properties.  
Front. Mech. Eng. 1:2.  
doi: 10.3389/fmech.2015.00002

<sup>1</sup> Department of Mechanical Engineering, Vasireddy Venkatadri Institute of Technology, Guntur, India, <sup>2</sup> Bioceramics and Coating Division, CSIR-Central Glass and Ceramic Research Institute (CGCRI), Kolkata, India, <sup>3</sup> Department of Mechanical Engineering, Andhra University College of Engineering, Visakhapatnam, India

Co-Cr-Mo alloy samples, fabricated using Laser Engineered Net Shaping – a laser-based additive manufacturing technology, have been subjected to heat treatment to study its influence on microstructure, wear, and corrosion properties. Following L9 Orthogonal array of Taguchi method, the samples were solutionized at 1200°C for 30, 45, and 60 min followed by water quenching. Aging treatment was done at 815 and 830°C for 2, 4, and 6 h. Heat treated samples were evaluated for their microstructure, hardness, wear resistance, and corrosion resistance. The results revealed that highest hardness of  $512 \pm 58$  Hv and wear rate of  $0.90 \pm 0.14 \times 10^{-4}$  mm<sup>3</sup>/N·m can be achieved with appropriate post-fabrication heat treatment. Analysis of variance and gray relational analysis on the experimental data revealed that the samples subjected to solution treatment for 60 min, without aging, exhibit best combination of hardness, wear, and corrosion resistance.

**Keywords:** additive manufacturing, laser engineered net shaping, Co-Cr-Mo, microstructure, wear, corrosion, heat treatment

## Introduction

Co-Cr-Mo alloys are well known for their high wear resistance and corrosion resistance. As they also exhibit good biocompatibility, they are widely used as surgical prostheses (Krishna et al., 2008; Bandyopadhyay et al., 2009; España et al., 2010; Dittrick et al., 2011). The microstructure and properties like wear resistance, hardness, etc., of Co-Cr-Mo alloy depends mainly on the carbon content and the type of heat treatment applied. Many researchers have applied different heat treatments to understand the mechanical behavior of Co-Cr-Mo alloys. In many heat treatment experiments, M<sub>23</sub>C<sub>6</sub> type carbides were observed to precipitate along the grain boundaries in the  $\gamma$  matrix of the alloy (Giacchi et al., 2011). In Ni and C free Co-Cr-Mo alloys, high heat treatment temperatures found to suppress  $\gamma$  (fcc) to  $\epsilon$  (hcp) martensitic transformation (Lee et al., 2005). Further, morphological change from lamellar to round carbides has been reported during solution and partial solution treatments of this alloy. Optimal results were obtained with solutionizing at 1120°C for 1 h followed by an aging at 815°C for 4 h (Bedolla-Gil et al., 2009).

As cast ASTM F75 – Co-Cr-Mo alloy usually exhibit two phase microstructure consisting of  $\sigma$ /M<sub>23</sub>C<sub>6</sub> and  $\sigma$ /Co- $\alpha$  eutectic (Rosenthal et al., 2010). The  $\pi$  phase has been identified in these alloys with carbon content between 0.15 and 0.35% after heat treatment at 1275°C

and holding times up to 0.5 h. Further complete dissolution of precipitates was observed in alloys with carbon contents  $<0.35\%$  (Mineta et al., 2010). When Co-Cr-Mo cast alloy samples were subjected to a solution heat treatment at  $1230^{\circ}\text{C}$  for 3 h followed by water quenching and isothermal aging at  $850^{\circ}\text{C}$  for different times, the samples exhibited lamellar type carbides ( $\gamma$  FCC +  $\text{M}_{23}\text{C}_6$ ) along the grain boundaries (Lashgari et al., 2011). Solution heat treatment carried out at  $1225^{\circ}\text{C}$  for 240 min on Co-Cr-Mo alloy resulted in blocky  $\text{M}_{23}\text{C}_6$  carbides in lamellar type matrix structures (Giacchi et al., 2012). Moreover, the microstructure of hot forged Co-Cr-Mo was found to be finer and exhibited superior mechanical properties compared to annealed alloys (Okazaki, 2008). Some reports are available on tribo-corrosion behavior of Co-Cr-Mo alloys (Ortega-Saenz et al., 2011; Pourzal et al., 2011; Mischler and Munoz, 2013). From these earlier studies, it is clear that no reported literature is available on the influence of heat treatment on microstructure, tribological, and corrosion properties of laser processed Co-Cr-Mo alloy.

Our earlier study on laser fabrication of Co-Cr-Mo alloy revealed that metallurgically sound, dense components can be obtained with a fine microstructure, when the process parameters are optimized (Mantrala et al., 2014). When compared with wrought Co-Cr-Mo alloy, the carbide volume fraction and the hardness were comparable, but the abrasive wear resistance of laser deposited alloy was found to be less (Janaki Ram et al., 2008). However, our preliminary studies on laser assisted additive manufacturing of Co-Cr-Mo alloy demonstrated that high laser power, low powder feed rate, and high scan speed can produce deposits with excellent mechanical, tribological, and electrochemical properties (Mantrala et al., 2014). In the present investigation, we aim to understand the influence of post-fabrication heat treatment on microstructure, hardness, wear, and corrosion properties of laser deposited Co-Cr-Mo alloy.

## Materials and Methods

Commercially available Co-Cr-Mo alloy (Stellite 21 – Kennametal Stellite, Goshen, IN, USA) powder was used to fabricate Co-Cr-Mo alloy using Laser Engineered Net Shaping (LENS™). Several deposits consisting of 5–8 layers and  $15\text{ mm}^2$  were fabricated at 350 W laser power, 5 g/min feed rate, and 20 mm/s scan speed to study the influence of post-fabrication heat treatment on microstructure, wear, and corrosion properties of this alloy. The above laser process parameters were optimized in our earlier study (Mantrala et al., 2014) and typical component fabricated using these parameters is shown in Figure 1.

L9 Orthogonal array of Taguchi method has been applied to optimize heat treatment cycle (Table 1). The Taguchi method provides minimum number of balanced experiments with small variance of results. All the samples were water quenched after solution heat treatment at  $1200^{\circ}\text{C}$ . The samples S1, S4, and S7 were restricted to solution treatment only whereas the other samples were subjected to aging at 815 and  $830^{\circ}\text{C}$  for different timings shown in Table 1.

The deposit hardness was measured using Vickers microhardness tester (MMT X7 MATSUZAWA) at 200 g load



**FIGURE 1 |** Additively manufactured Co-Cr-Mo alloy impeller using Laser Engineered Net Shaping (LENS™).

**TABLE 1 |** Experimental parameters used in the present investigation.

Sample no.	Solution treatment time (min)	Aging temperature ( $^{\circ}\text{C}$ )	Aging time (h)
S1	30	No aging	
S2	30	815	4
S3	30	830	6
S4	45	No aging	
S5	45	815	6
S6	45	830	2
S7	60	No aging	
S8	60	815	2
S9	60	830	4

applied for 20 s. An average of 10 measurements on 3 identical samples was reported. The constituent microstructural phases of laser deposited Co-Cr-Mo alloy were determined using an X'Pert Pro MPD diffractometer (PANalytical) operating at 45 kV and 40 mA using Ni-filtered  $\text{CuK}\alpha$  radiation. The microstructures of the samples were analyzed using scanning electron microscope (ProX, Phenom-World BV, Eindhoven, Netherlands).

Electrochemical measurements were performed on heat treated Co-Cr-Mo alloy samples using a potentiostat/galvanostat (SP300, Bio-Logic SAS, France) in 3.5% NaCl solution. Before testing, the top surfaces of the deposits were polished up to  $1\ \mu\text{m}$   $\text{Al}_2\text{O}_3$ . Potentiodynamic polarization tests were performed (on three identical samples) by scanning the applied potential from  $-0.5$  to  $1.6\text{ V}$  vs. saturated calomel electrode (SCE) at a rate of  $10\text{ mV/min}$ . The corrosion potential ( $E_{\text{corr}}$ ) and the corrosion current density ( $I_{\text{corr}}$ ) was extracted from the polarization curves of the linear part of the cathodic curve (Tafel behavior).

Ball on disk wear tests were performed on the samples using a tribometer (NANOVEA, Microphotonics Inc., CA, USA) under a normal load of 10 N for 1000 m sliding distance. An  $\text{Al}_2\text{O}_3$

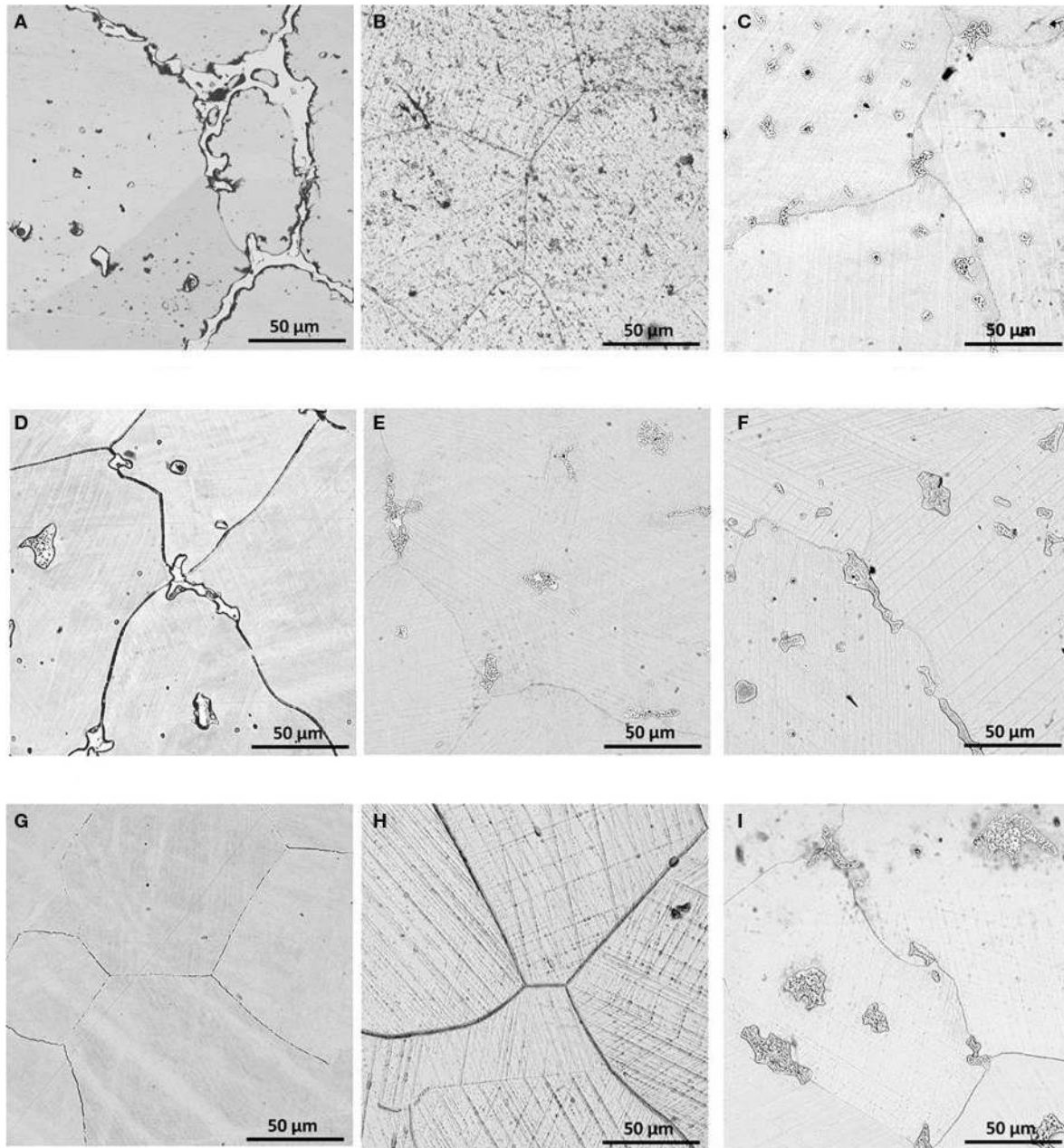


**FIGURE 2 |** Microstructure of Co-Cr-Mo alloy samples solutionized at 1200° C for different times followed by aging (A) S1-30 min, no aging; (B) S2-30 min, 815°C, 4 h; (C) S3-30 min, 830°C, 6 h; (D) S4-45 min,

no aging; (E) S5-45 min, 815°C, 6 h; (F) S6-45 min, 830°C, 2 h; (G) S7-60 min, no aging; (H) S8-60 min, 815°C, 2 h; (I) S9-60 min, 830°C, 4 h.

ball of 3 mm diameter was used as counter body. The wear tests were carried out on three samples processed at each heat treatment condition (S1–S9). The wear rate of the deposits was calculated from the wear track measurements and was represented as  $\text{mm}^3/\text{N}\cdot\text{m}$ . The wear tracks were observed using SEM to understand the wear mechanism.

Analysis of variance (ANOVA) was performed on the hardness, wear rate, and corrosion data. In the present work, we aim at identifying optimum heat treatment parameters, which can

provide high corrosion resistance along with high hardness and wear resistance. For this purpose, the multiple responses (hardness, wear rate,  $E_{\text{CORR}}$ , and low  $I_{\text{CORR}}$ ) have been converted in to a single index using gray relational grade analysis (Deng, 1989). It is known that a material with more positive  $E_{\text{CORR}}$  and low  $I_{\text{CORR}}$  exhibit high corrosion resistance. Therefore, we have used “higher the better” for  $E_{\text{CORR}}$  and hardness, and “lower the better” for  $I_{\text{CORR}}$  and wear rate for normalization. Following equations were used to calculate the gray relational grade (Deng, 1989).



## Normalization of Response

$$\text{Higher the better} = N_i(R) = \frac{\nu_i(R) - \nu_i(R)(\min)}{\nu_i(R)(\max) - \nu_i(R)(\min)} \quad (1)$$

$$\text{Lower the better} = N_i(R) = \frac{\nu_i(R)(\max) - \nu_i(R)}{\nu_i(R)(\max) - \nu_i(R)(\min)} \quad (2)$$

where  $N_i(R)$  is the normalized response,  $\nu_i(R)$  is the experimental value of  $R$ th response (in the present work the responses were hardness, wear rate,  $E_{\text{corr}}$  and  $I_{\text{corr}}$ ),  $\nu_i(R)(\max)$  and  $\nu_i(R)(\min)$  are maximum and minimum experimental values of  $R$ th response.

## Gray Relational Coefficient

The normalized response [ $N_i(R)$ ] was used to calculate gray relational coefficient as follows:

$$\alpha(R) = \frac{\Delta_{\min} + 0.5\Delta_{\max}}{\Delta\nu_i(R) + 0.5\Delta_{\max}} \quad (3)$$

where  $\Delta\nu_i(R) = 1 - N_i(R)$ ,  $\Delta_{\min}$  and  $\Delta_{\max}$  are the minimum and maximum values of  $\Delta\nu_i(R)$  (for  $R$ th response).

## Gray Relational Grade

The final grading of combined effect of responses was done with gray relational grade as follows:

$$\text{GRG} = \frac{1}{n} \sum_{R=i}^n \alpha(R) \quad (4)$$

where  $n$  is the number of responses (in the present work the responses were hardness, wear rate,  $E_{\text{corr}}$ , and  $I_{\text{corr}}$ , i.e.,  $n = 4$ ). The highest grade indicates the best combination of process parameters for high hardness and  $E_{\text{corr}}$ , and low wear rate and  $I_{\text{corr}}$ .

## Results and Discussion

The microstructures of laser deposited Co-Cr-Mo alloy heat treatment (S1–S9) are shown in Figure 2. In general, all samples showed equiaxed Co grains with or without carbide precipitates depending on heat treatment conditions. However, heat treatments found have no measurable influence on grain size of laser fabricated Co-Cr-Mo alloy. The carbides precipitates were observed not only along the boundaries but also within the grains. The precipitates found to decrease in size and amount with increasing solutionizing time from 30 to 60 min, as shown in Figures 2A,D,G. At solutionizing temperature of 1200°C, increasing the holding time allow more diffusion and carbides can dissolve in the matrix and therefore the concentration of precipitates decreased in Co-Cr-Mo alloy with increasing solutionizing time. As expected, increasing the aging time from 2 h (Figure 2F) to 4 h (Figure 2I), at 830°C aging temperature, increased the precipitation and is attributed to decrease in solid solubility of carbide elements in Co matrix. Similarly, the increasing the aging temperature increased the precipitation concentration as shown in Figure 2C (S3-30 min, 830°C, 6 h) and Figure 2E (S5-45 min, 815°C, 6 h). X-ray diffraction data, Figure 3, confirmed the presence of carbide precipitates in most of Co-Cr-Mo alloy samples. The precipitates were identified

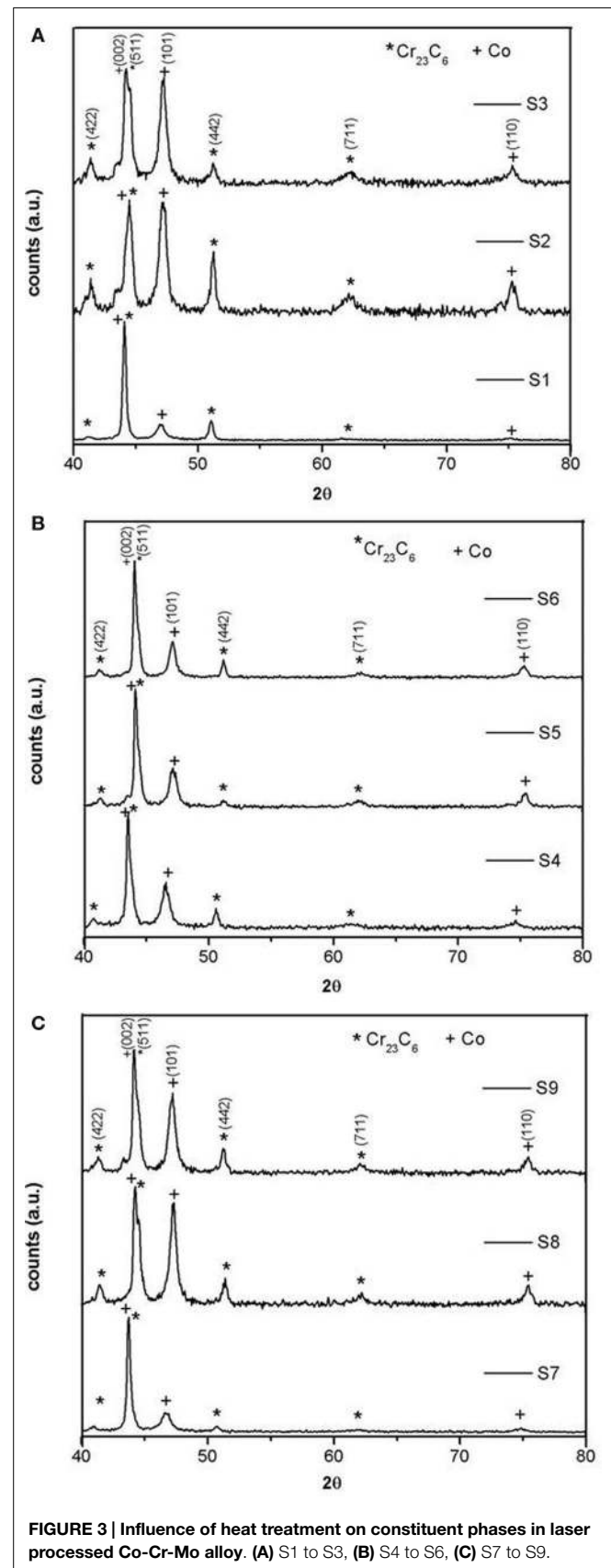


**FIGURE 3 | Influence of heat treatment on constituent phases in laser processed Co-Cr-Mo alloy. (A) S1 to S3, (B) S4 to S6, (C) S7 to S9.**

**TABLE 2 | Experimentally determined hardness, wear rate, and corrosion data of laser fabricated Co-Cr-Mo alloy.**

Sample ID	Hardness (Hv)	Wear rate ( $\times 10^{-4}$ mm <sup>3</sup> /N·m)	Corrosion		Gray relational analysis	
			$I_{corr}$ ( $\mu$ A/cm <sup>2</sup> )	$E_{corr}$ (mV vs. SCE)	Grade	Order
S1	491 ± 51	1.44 ± 0.28	0.11	-368	0.563	7
S2	382 ± 25	1.18 ± 0.24	0.20	-300	0.463	9
S3	378 ± 11	1.19 ± 0.25	0.22	-61	0.514	8
S4	372 ± 44	0.96 ± 0.28	0.42	+64	0.624	3
S5	386 ± 25	1.17 ± 0.12	0.44	+85	0.568	6
S6	512 ± 58	1.08 ± 0.18	0.28	-116	0.670	2
S7	478 ± 81	0.96 ± 0.25	0.05	-178	0.739	1
S8	484 ± 37	0.97 ± 0.13	0.61	-86	0.603	5
S9	380 ± 35	0.90 ± 0.14	0.39	-22	0.619	4

Gray relational grade and its order are presented in the last column.

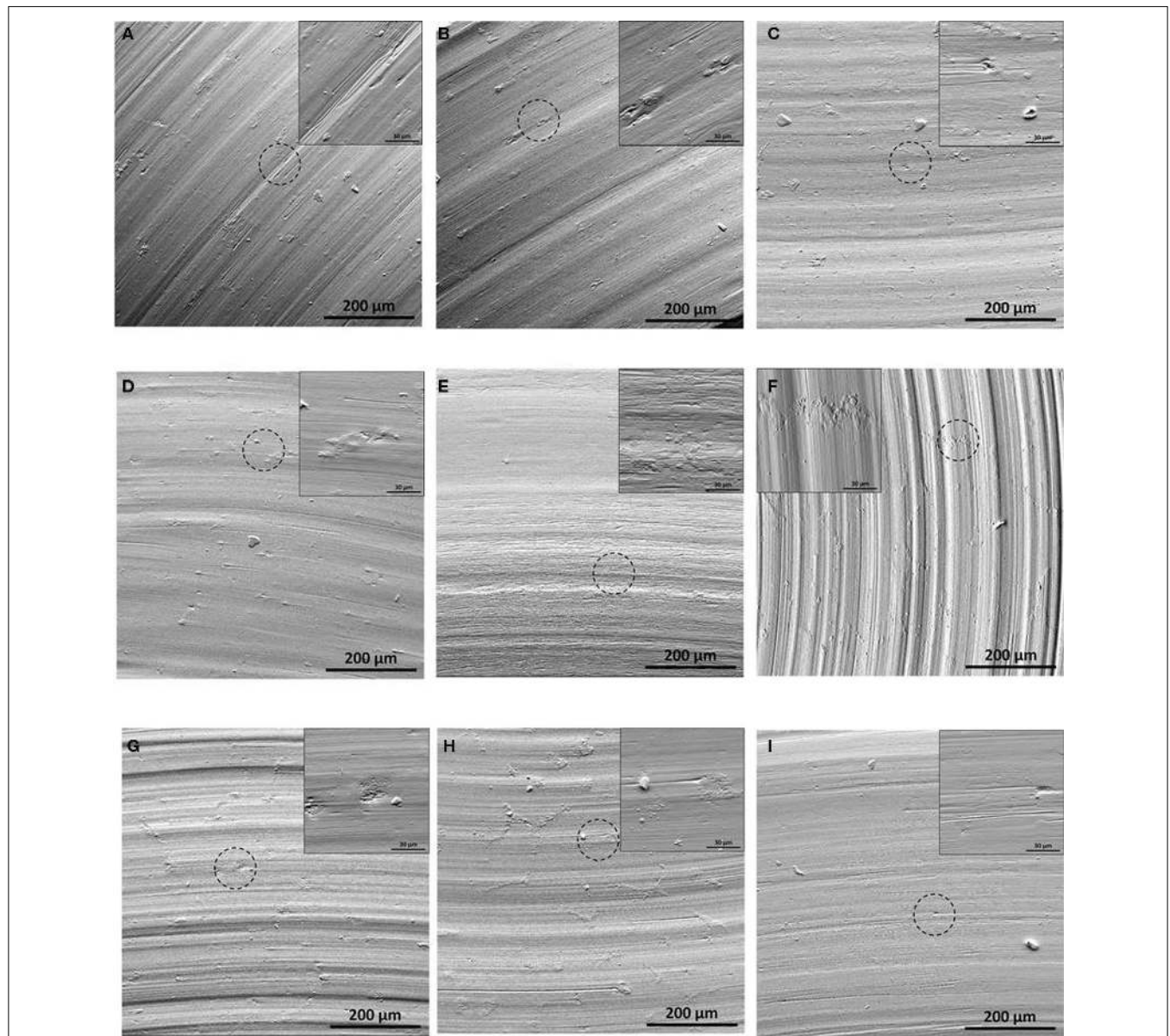


**FIGURE 4 | Wear track morphologies of Co-Cr-Mo alloy samples (A-I) S1-S9. Inset shows magnified image of region highlighted with circle.**

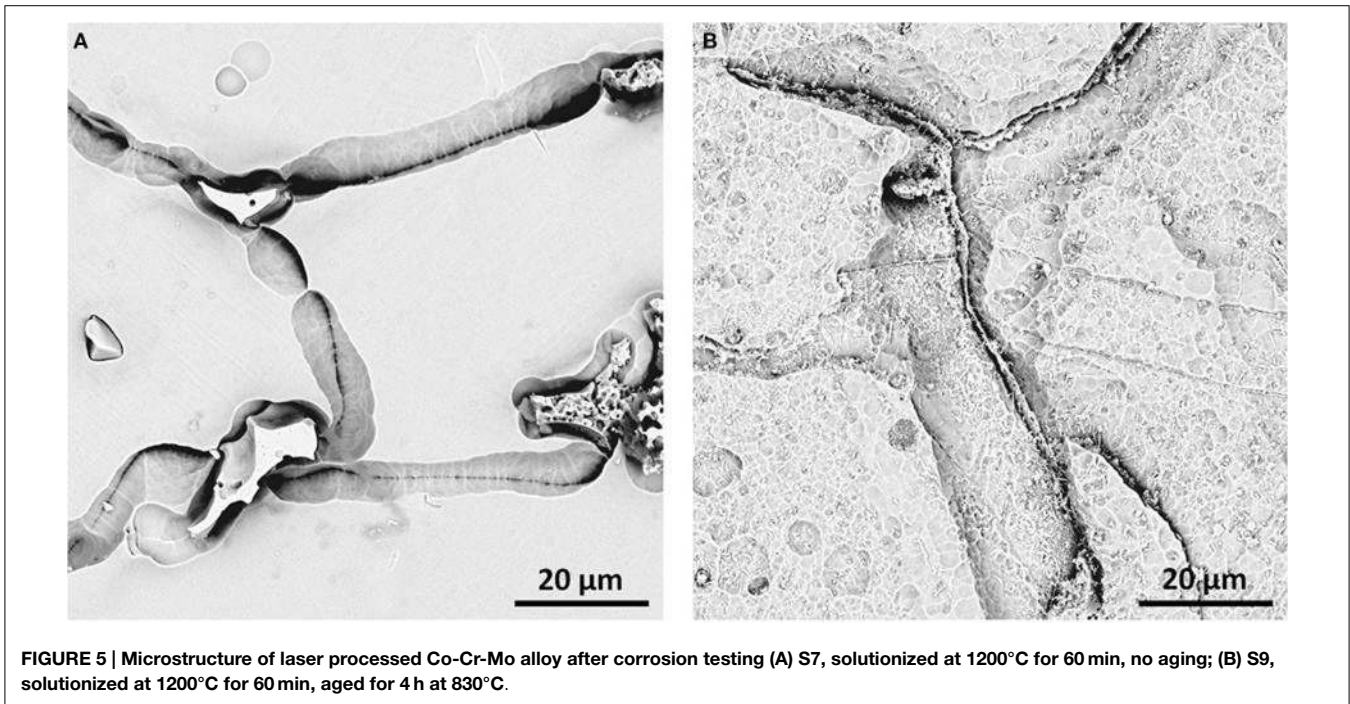


**FIGURE 5 |** Microstructure of laser processed Co-Cr-Mo alloy after corrosion testing (A) S7, solutionized at 1200°C for 60 min, no aging; (B) S9, solutionized at 1200°C for 60 min, aged for 4 h at 830°C.

as  $\text{Cr}_{23}\text{C}_6$  precipitates and the aging treatment increased their peak intensities. This observation indicates that the precipitation increased with increasing aging time and temperature. The XRD results also confirmed the absence of any other type of carbides in laser fabricated Co-Cr-Mo alloy.

The influence of heat treatment on hardness of Co-Cr-Mo alloy is presented in Table 2. Although the microstructures and XRD showed some clear trend with solutionizing time, aging temperature, and time, mixed trend was observed for hardness. Some samples (S2, S3, S4, S5, and S9) showed low hardness between 372 and 386 Hv, whereas other samples (S1, S6, S7, and S8) exhibited high hardness in the range of 478–512 Hv. Highest hardness of  $512 \pm 58$  Hv was recorded for samples, which were solutionized for 45 min at 1200°C followed by aging at 830°C for 2 h. However, tribological testing showed lowest wear rate ( $0.90 \pm 0.14 \times 10^{-4} \text{ mm}^3/\text{N}\cdot\text{m}$ ) with heat treatment cycle of 60 min at 1200°C followed by aging at 830°C, 4 h. While the sample, which exhibited high hardness of  $491 \pm 51$  Hv found to have high wear rate of  $1.44 \pm 0.28 \times 10^{-4} \text{ mm}^3/\text{N}\cdot\text{m}$  during tribological testing. This discrepancy is presumably due to variations in precipitate size and their distribution as a result of post-fabrication heat treatment. In general, the samples subjected to longer solutionizing times (S7, S8, S9) exhibited high wear resistance compared to other samples, which could be due to complete dissolution and re-precipitation of carbides during solutionizing and aging treatments, respectively. The wear track morphologies of Co-Cr-Mo alloy samples are presented in Figure 4. All samples showed deep grooves with third body wear characteristics. The samples with low wear rate exhibited smoother wear tracks than other samples with high wear rate. For example, the sample S4 (solutionized for 45 min at 1200°C) and S9 (solutionized for 60 min at 1200°C and aged 830°C for 4 h) showed

**TABLE 3 |** Influence of heat treatment parameters on hardness, wear, and corrosion resistance.

Response	Solution time	Aging temperature	Aging time
Hardness (%)	5	5	77
Wear resistance (%)	71	2	14
Corrosion resistance (%)	13	27	57
Overall (%)	56	29	5

clearly smoother wear tracks (Figures 4D,I) compared to other samples. Further, in all samples carbide pullout was observed as shown in insets of Figures 4D,G. These pulled out carbide particles entrapped between articulating substrate and  $\text{Al}_2\text{O}_3$  ball resulted in third body wear.

The corrosion potential ( $E_{\text{corr}}$ ) and corrosion current ( $I_{\text{corr}}$ ) of Co-Cr-Mo alloy samples derived from respective Tafel plots are summarized in Table 2. It is well known that the materials exhibit high corrosion resistance if  $E_{\text{corr}}$  values tend to be positive with minimum possible  $I_{\text{corr}}$  values. Our experimental results show that  $I_{\text{corr}}$  values decreased from  $4.63 \mu\text{A}/\text{cm}^2$  (un-heat treated samples) (Mantrala et al., 2014) to the range of  $0.05\text{--}0.61 \mu\text{A}/\text{cm}^2$  after heat treatment, while mixed results were observed with  $E_{\text{corr}}$  values. Evidently, the corrosion rate is relatively lower than untreated samples (Mantrala et al., 2014). As shown in Figure 5, the corrosion was found to be localized primarily along grain boundaries. In addition, the corrosion was more pronounced around the carbide precipitates. This is primarily due to reduction in Cr in the matrix as a result of carbide precipitation. To study the combined effect of  $I_{\text{corr}}$  and  $E_{\text{corr}}$ , Gray Relational Analysis has been carried out and the results revealed that samples



solutionized at 1200°C for 45 min without aging would provide highest corrosion resistance for laser fabricated Co-Cr-Mo alloy.

The percentage contribution of heat treatment parameters toward hardness, wear rate, and corrosion resistances was calculated using ANOVA and tabulated in Table 3. The data indicated that heat treatment parameters have strong influence on properties of laser fabricated Co-Cr-Mo alloy. The aging time had highest influence of 77% on hardness and 57% on corrosion resistance. Whereas the most influential factor for wear resistance was solutionizing time with 71%. For example, samples those were not subjected to aging (or aged for shorter times) exhibited high hardness and high corrosion resistance (S1, S6, S7, and S8). Similarly, irrespective of aging time, the samples subjected to longer solution times have exhibited high wear resistance (S7, S8, and S9). Based on above discussion for high hardness, high wear resistance, and high corrosion resistance samples S6, S9, and S7 are the best, respectively. To identify the best heat treatment parameters for best combination of high hardness, high wear resistance, and high corrosion resistance the gray relational analysis was used. The analysis showed that laser fabricated Co-Cr-Mo alloy can provide best combination of hardness, wear, and corrosion resistance if a solution treatment at 1200°C for 60 min is given. In summary, the solutionizing time found to have stronger influence followed

by aging temperature and time on overall performance of the Co-Cr-Mo alloy.

## Conclusions

In this work, we have successfully fabricated net shape Co-Cr-Mo alloy impeller using laser based additive manufacturing technology. Microstructural analysis showed complete carbide dissolution with increasing solutionizing time and their precipitation with aging temperature and time. Overall, the heat treatment found to improve properties of laser fabricated Co-Cr-Mo alloy. The samples solutionized at 1200°C for 45 min followed by aging at 830°C for 2 h exhibited highest hardness. Tribological tests on these samples revealed that solutionizing treatment at 1200°C for 60 min with 4 h aging at 830°C results in significant improvement in wear resistance of this alloy.

## Acknowledgments

The authors would like to acknowledge the financial support from the Council of Scientific and Industrial Research (CSIR), New Delhi to establish LENS™ facility at CSIR-CGCRI and through project ESC0103. Mr. KM Mantrala is grateful to the Director, CSIR-CGCRI, Kolkata for granting permission to carry out some of the experimental and characterization work at CSIR-CGCRI.

## References

- Bandyopadhyay, A., Krishna, B. V., Xue, W., and Bose, S. (2009). Application of laser engineered net shaping (LENS) to manufacture porous and functionally graded structures for load bearing implants. *J. Mater. Sci. Mater. Med.* 20(Suppl. 1), S29–S34. doi:10.1007/s10856-008-3478-2
- Bedolla-Gil, Y., Juarez-Hernandez, A., Perez-Unzueta, A., Garcia-Sanchez, E., Mercado-Solis, R., and Hernandez-Rodriguez, M. A. L. (2009). Influence of heat treatments on mechanical properties of a biocompatibility alloy ASTM F75. *Rev. Mex. Fis.* 55, 1–5.
- Deng, J. (1989). Introduction to grey system. *J. Grey Syst.* 1, 1–24.
- Dittrick, S., Balla, V. K., Davies, N. M., Bose, S., and Bandyopadhyay, A. (2011). In vitro wear rate and Co Ion release of compositionally and structurally graded CoCrMo-Ti6Al4V structures. *Mater. Sci. Eng. C* 31, 809–814. doi:10.1016/j.msec.2010.07.009
- España, F. A., Balla, V. K., Bose, S., and Bandyopadhyay, A. (2010). Design and fabrication of CoCrMo based novel structures for load bearing implants using laser engineered net shaping. *Mater. Sci. Eng. C* 30, 50–57. doi:10.1016/j.msec.2009.08.006
- Giacchi, J. V., Fornaro, O., and Palacio, H. (2012). Microstructural evolution during solution treatment of Co-Cr-Mo-C biocompatible alloys. *Mater. Charact.* 68, 49–57. doi:10.1016/j.matchar.2012.03.006
- Giacchi, J. V., Morando, C. N., Fornaro, O., and Palacio, H. A. (2011). Microstructural characterization of as-cast biocompatible Co-Cr-Mo alloys. *Mater. Charact.* 62, 53–61. doi:10.1016/j.matchar.2010.10.011
- Janaki Ram, G. D., Esplin, C. K., and Stucker, B. E. (2008). Microstructure and wear properties of LENS deposited medical grade CoCrMo. *J. Mater. Sci. Mater. Med.* 19, 2105–2111. doi:10.1007/s10856-007-3078-6
- Krishna, B. V., Xue, W., Bose, S., and Bandyopadhyay, A. (2008). Functionally graded Co-Cr-Mo coating on Ti-6Al-4V alloy structures. *Acta Biomater.* 4, 697–706. doi:10.1016/j.actbio.2007.10.005
- Lashgari, H. R., Zangeneh, S. H., and Ketabchi, M. (2011). Isothermal aging effect on the microstructure and dry sliding wear behavior of Co-28Cr-5Mo-0.3C alloy. *J. Mater. Sci.* 46, 7262–7274. doi:10.1007/s10853-011-5686-2
- Lee, S.-H., Takahashi, E., Nomura, N., and Chiba, A. (2005). Effect of heat treatment on microstructure and mechanical properties of Ni- and C-free Co-Cr-Mo alloys for medical applications. *Mater. Trans.* 46, 1790–1793. doi:10.2320/matertrans.46.1790
- Mantrala, K. M., Das, M., Balla, V. K., Rao, Ch. S., and Kesava Rao, V. V. S. (2014). Laser-deposited CoCrMo alloy: microstructure, wear and electrochemical properties. *J. Mater. Res.* 29, 2011–2027. doi:10.1557/jmr.2014.163
- Mineta, S., Namba, S., Yoneda, T., Ueda, K., and Narushima, T. (2010). Carbide formation and dissolution in biomedical Co-Cr-Mo alloys with different carbon contents during solution treatment. *Metall. Mater. Trans. A* 41A, 2129–2138. doi:10.1007/s11661-010-0227-1
- Mischler, S., and Munoz, A. I. (2013). Wear of CoCrMo alloys used in metal-on-metal hip joints: a tribocorrosion appraisal. *Wear* 297, 1081–1094. doi:10.1016/j.wear.2012.11.061
- Okazaki, Y. (2008). Effects of heat treatment and hot forging on microstructure and mechanical properties of Co-Cr-Mo alloy for surgical implants. *Mater. Trans.* 49, 817–823. doi:10.2320/matertrans.MRA2007299
- Ortega-Saenz, J. A., Hernandez-Rodriguez, M. A. L., Ventura-Sobrevilla, V., Michalczewski, R., Smolik, J., and Szczerek, M. (2011). Tribological and corrosion testing of surface engineered surgical grade CoCrMo alloy. *Wear* 271, 2125–2131. doi:10.1016/j.wear.2010.12.062
- Pourzal, R., Catelas, I., Theissmann, R., Kaddick, C., and Fischer, A. (2011). Characterization of wear particles generated from CoCrMo alloy under sliding wear conditions. *Wear* 271, 1658–1666. doi:10.1016/j.wear.2010.12.045
- Rosenthal, R., Cardoso, B. R., Bott, I. S., Paranhos, R. P. R., and Carvalho, E. A. (2010). Phase characterization in as-cast F-75 Co-Cr-Mo-C alloy. *J. Mater. Sci.* 45, 4021–4028. doi:10.1007/s10853-010-4480-x

**Conflict of Interest Statement:** The authors declare that the research was conducted in the absence of any commercial or financial relationships that could be construed as a potential conflict of interest.

Copyright © 2015 Mantrala, Das, Balla, Rao and Kesava Rao. This is an open-access article distributed under the terms of the Creative Commons Attribution License (CC BY). The use, distribution or reproduction in other forums is permitted, provided the original author(s) or licensor are credited and that the original publication in this journal is cited, in accordance with accepted academic practice. No use, distribution or reproduction is permitted which does not comply with these terms.